Acta Crystallographica Section F
Structural Biology and Crystallization Communications
ISSN 1744-3091

Crystallization and preliminary X-ray analysis of the RXLR-type effector RXLR3 from the oomycete pathogen *Hyaloperonospora arabidopsidis*

Lennart Wirthmueller,[a] Jonathan D. Jones[b] and Mark J. Banfield[a]*

[a]Department of Biological Chemistry, John Innes Centre, Norwich Research Park, Norwich NR4 7UH, England, and [b]The Sainsbury Laboratory, John Innes Centre, Norwich Research Park, Norwich NR4 7UH, England

Correspondence e-mail: mark.banfield@jic.ac.uk

Received 3 August 2011
Accepted 2 September 2011

Manipulating defence responses in infected host cells is a prerequisite for filamentous plant pathogens to complete their life cycle on infected host plants. During infection of its host *Arabidopsis thaliana*, the oomycete pathogen *Hyaloperonospora arabidopsidis* secretes numerous RXLR-type effector proteins, some of which are translocated into host cells. RXLR-type effectors share conserved N-terminal translocation motifs but show high diversity in their C-terminal 'effector domains' that manipulate host defence mechanisms. Therefore, obtaining structural information on the effector domains of RXLR-type effectors will contribute to elucidating their molecular-virulence functions in infected host cells. Here, the expression, purification and crystallization of the effector domain of RXLR3 from *H. arabidopsidis* isolate Waco9 are reported. The crystals belonged to space group $P2_12_12$, with unit-cell parameters $a = 61.49$, $b = 27.99$, $c = 37.59$ Å. X-ray data were collected to a resolution of 1.8 Å from a single crystal using synchrotron radiation.

1. Introduction

Following successful penetration of the plant cuticle, filamentous pathogens such as oomycetes further invade the host tissue by forming hyphae and develop specialized feeding structures called haustoria that constitute an intimate interface between the pathogen and infected host cells (Panstruga & Dodds, 2009). Post-invasive growth is antagonized by basal plant-defence mechanisms (Lipka *et al.*, 2005). Therefore, successful oomycetes secrete a variety of effector proteins that act outside or inside host cells to suppress plant defence. In turn, plant immune receptors monitor the presence of effector proteins secreted by pathogens and upon recognition potentiate plant defences to restrict pathogen spread (Eitas & Dangl, 2010). Understanding how secreted effector proteins evade recognition and suppress plant defence is thus essential to understand the virulence mechanisms that make oomycetes such successful pathogens and is a prerequisite to enhance plant resistance towards oomycetes.

Most of the oomycete effector proteins characterized to date have a modular domain architecture. An N-terminal signal peptide mediates secretion *via* the eukaryotic secretory pathway. Downstream of the signal peptide, bioinformatic analysis revealed a conserved motif dubbed 'RXLR' (arginine, any amino acid, leucine, arginine) in many oomycete effectors. Mutations in the RXLR motifs of the *Phytophthora* effectors AVR3a (*P. infestans*) and AVR1b (*P. sojae*) impair translocation into host cells (Whisson *et al.*, 2007; Dou *et al.*, 2008). Therefore, the RXLR motif may have a conserved function in delivering pathogen effectors into plant cells. The region downstream of the translocation motifs is often referred to as the 'effector domain' because it is sufficient and required for defence suppression when effector proteins are directly delivered into host cells (Sohn *et al.*, 2007). Consistent with these findings, effector families that are under positive selection show a bias of non-synonymous substitutions towards the effector domain, whereas the N-terminal translocation signals are often conserved (Allen *et al.*, 2004, 2008). Taken together, these results suggest that the defence-suppressing activity of

oomycete effectors is mediated by the region downstream of the translocation motifs.

The oomycete *Hyaloperonospora arabidopsidis* is a natural obligate biotrophic pathogen on *Arabidopsis thaliana* (Slusarenko & Schlaich, 2003). The *H. arabidopsidis* and *Arabidopsis* genomes have been annotated, making this pathosystem a useful tool to understand how oomycete effectors suppress plant defence. RXLR-type candidate effectors from *H. arabidopsidis* have been cloned and their effector domains have been tested for virulence activity by expression in plant cells (Fabro *et al.*, 2011). As most candidate effectors lack significant sequence similarity to proteins of known function, gaining structural information on *H. arabidopsidis* effector domains will contribute to understanding their virulence functions. Moreover, three-dimensional structures will provide useful frameworks for mutagenesis studies once target proteins of the effector have been identified. Recent work from our group and others has identified a conserved helix-bundle fold in several RXLR-type effector proteins from different oomycete species that appears to be a modular building block for effector domains (Boutemy *et al.*, 2011; Yaeno *et al.*, 2011; Chou *et al.*, 2011). Here, we report the expression, purification and crystallization of the effector domain of *H. arabidopsidis* RXLR3, which lacks the conserved amino-acid motifs found in helix-bundle effector domains and might therefore adopt a different fold. RXLR3 was identified in an expressed sequence-tag library from *Arabidopsis* tissue infected with *H. arabidopsidis* race Waco9 (Cabral *et al.*, 2011). RXLR3 is present in seven different *H. arabidopsidis* races that have been analyzed and shows only weak evidence of positive selection (Cabral *et al.*, 2011). Conceivably, RXLR3 may belong to a core set of *H. arabidopsidis* effectors that have been selected during co-evolution with its host. Determination of the crystal structure of the RXLR3 effector domain should provide further structural insights into RXLR-type effector folds.

2. Materials and methods

2.1. Protein expression, purification and crystallization

Bioinformatic analysis predicted a 19-amino-acid N-terminal signal peptide for RXLR3 (GenBank accession No. AEF57433.1; signal peptide probability 0.998 from *SignalP* 3.0; Emanuelsson *et al.*, 2007). At positions 49–54 the amino-acid sequence RHLR is followed by two glutamic acid residues, suggesting that the RXLR3 effector domain starts after Glu54. Consistently, the prediction of disordered regions using *RONN* (Yang *et al.*, 2005) suggested that amino acids Met1–Glu53 are likely to be disordered, followed by a predicted ordered region from Glu54 to Asp120. The nine C-terminal amino acids were predicted to be disordered. We concluded that the region between Glu54 and the C-terminal residue Phe129 is most likely to constitute the RXLR3 effector domain. A sequence encoding amino acids Val55–Phe129 was amplified by PCR using primers R3f (AAGTTCTGTTTCAGGGCCCGgttgggcctgagacttt) and R3r (ATGGTCTAGAAAGCTTTAgaaacgatgcgggcggc) and cloned between the *Kpn*I and *Hin*dIII sites of pOPINF (Berrow *et al.*, 2007) using In-Fusion HD enzyme (Clontech) to generate a fusion protein with an N-terminal hexahistidine (His_6) tag and a 3C protease cleavage site. After cleavage of the His_6 tag by 3C protease, this cloning strategy resulted in two additional amino acids (Gly-Pro) remaining at the N-terminus of the protein used for crystallization experiments. The construct was transformed into *Escherichia coli* SoLuBL21 DE3 cells (Genlantis). Expression was induced at an OD of 0.8 with 0.5 m*M* IPTG and the cells were shaken at 200 rev min^{-1} for 5 h at 298 K. The cells were harvested by centrifugation and resuspended in buffer *A* (50 m*M* HEPES, 300 m*M* NaCl, 25 m*M* imidazole pH 7.8). Following incubation at 298 K for 20 min, the cells were sonicated for a total time of 2 min with 40% amplitude on a Vibra-Cell sonicator (Sonics). Cell debris was removed by centrifugation at 30 000*g* for 30 min. Soluble His_6-RXLR3 protein was purified from the supernatant on an ÄKTAxpress purifier. The soluble protein extract was loaded onto a 5 ml HisTrap column (Amersham Pharmacia) and washed with ten column volumes of buffer *A*. His_6-RXLR3 was eluted with buffer *B* (50 m*M* HEPES, 300 m*M* NaCl, 250 m*M* imidazole pH 7.8) and the eluted proteins were subjected to size-exclusion chromatography on a HiLoad 16/60 Superdex 75 column (Amersham Pharmacia) equilibrated with gel-filtration buffer (20 m*M* HEPES, 150 m*M* NaCl pH 7.5). Fractions containing His_6-RXLR3 were pooled and concentrated to approximately 8 mg ml^{-1} using Vivaspin ultrafiltration columns with a molecular-weight cutoff of 5000 Da (Sartorius) and incubated with 3C protease for 24 h at 277 K to cleave the His_6 tag. The His_6 tag and His_6-tagged 3C protease were removed by passing the proteins through a 5 ml HisTrap column. RXLR3 protein that passed through the column was subjected to a second size-exclusion chromatography step (as above) and the protein was concentrated to 30 mg ml^{-1} using Vivaspin columns.

All crystallization experiments were carried out at 293 K and at a protein concentration of 8 mg ml^{-1}. An initial screen for crystallization conditions was performed in MRC sitting-drop plates (Molecular Dimensions) by mixing 600 nl protein solution and 600 nl reservoir solution using a Oryx Nano robot (Douglas Instruments). Optimization of the initial crystals was carried out in hanging-drop plates (Molecular Dimensions) by mixing 1.5 µl protein solution with an equal amount of reservoir solution.

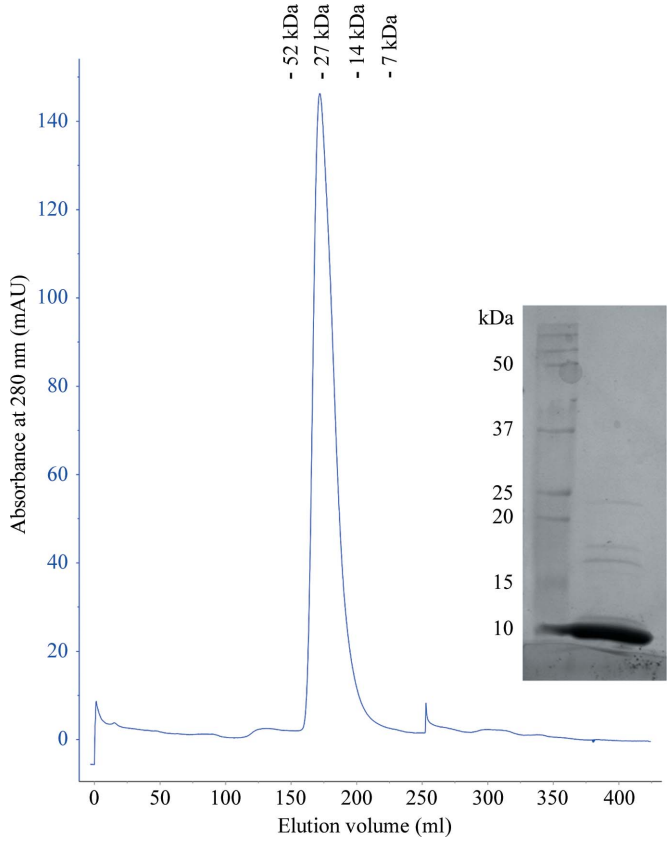

Figure 1
Size-exclusion chromatogram and SDS–PAGE analysis (inset) of RXLR3. The gel was stained with Coomassie Brilliant Blue.

2.2. X-ray data collection

For data collection, rod clusters were broken by punching their centre with an acupuncture needle and single crystals were mounted in LithoLoops (Molecular Dimensions). The crystals were transferred to a cryoprotectant solution [crystallization solution supplemented with 25%(*v*/*v*) glycerol] and flash-frozen in liquid nitrogen until data collection. Diffraction data were collected using an ADSC Quantum 315 CCD detector on station I02 of the Diamond Light Source (Oxfordshire, UK) with the wavelength set to 0.91 Å. The crystal was maintained at a cryogenic temperature with a Cryojet cryocooler (Oxford Instruments). Diffraction data were processed using *iMOSFLM* (Battye *et al.*, 2011) and *SCALA* (Evans, 2006).

3. Results and discussion

His_6-RXLR3 protein could be expressed in *E. coli* SoLuBL21 DE3 cells and purified with a typical yield of ∼4 mg per litre of culture medium. The RXLR3 protein constituted >95% of the sample as judged by SDS–PAGE analysis (Fig. 1). The intact monoisotopic mass of the RXLR3 protein was determined to be 8727.80 Da, which was consistent with the calculated molecular mass of 8727.74 Da. On size-exclusion chromatography the protein eluted with a retention volume that corresponded to a molecular mass of approximately 27 kDa, suggesting that RXLR3 may form dimers or other higher order oligomers. In accordance with this finding, RXLR3 interacts with itself when assayed in a yeast two-hybrid system (Mukhtar *et al.*, 2011).

Figure 2
Clusters of plate-like crystals of RXLR3.

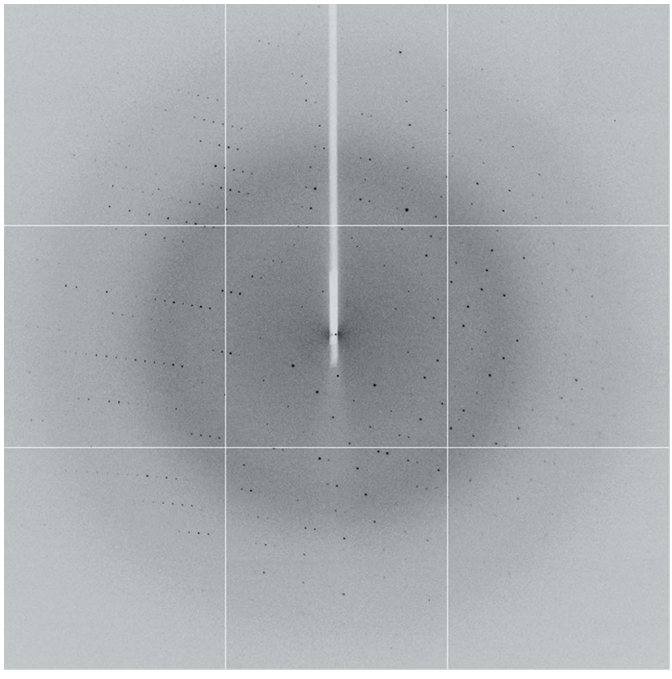

Figure 3
X-ray diffraction image from a crystal of RXLR3.

Table 1
Summary of X-ray data for RXLR3 (the reported data-collection statistics were calculated using *SCALA*).

Values in parentheses are for the outer resolution shell.

No. of crystals	1
Beamline	I02, Diamond Light Source, UK
Wavelength (Å)	0.91
Crystal-to-detector distance (mm)	279.8
Rotation range per image (°)	1.0
Total rotation range (°)	1000
Resolution range (Å)	37.0–1.8 (1.9–1.8)
Space group	$P2_12_12$
Unit-cell parameters (Å)	a = 61.49, b = 27.99, c = 37.59
Mosaicity (°)	1.20
Total No. of measured intensities	217435 (29871)
Unique reflections	6418 (908)
Multiplicity (full data set/half data set)	33.9 (32.9)/18.5 (17.4)
Mean $I/\sigma(I)$	29.5 (8.9)
Completeness (full data set/half data set) (%)	99.8 (99.9)/100.0 (99.9)
R_{merge}	0.091 (0.422)
ΔAnom correlation between half sets	0.654
Mid-Slope of Anom Normal Probability	1.525

Crystallization trials were carried out using various commercially available screens. RXLR3 crystallized in a single plate cluster in one condition (2.2 *M* ammonium sulfate, 0.2 *M* ammonium bromide; AmSO4 suite from Qiagen, condition No. 16). Optimizing the crystallization conditions to 0.1 *M* MES, 2.0 *M* ammonium sulfate, 0.2 *M* ammonium bromide pH 6.0 gave rise to clusters of more defined and thicker plates (Fig. 2).

These crystals diffracted to a resolution of 1.8 Å on station I02 of the Diamond Light Source (Fig. 3). A total of 1000° of data were collected with 1° oscillations in φ. Indexing the collected data using *iMOSFLM* suggested a primitive orthorhombic lattice for the crystals, with unit-cell parameters a = 61.49, b = 27.99, c = 37.59 Å. The systemic absences (analyzed with *POINTLESS*; Evans, 2006) and scaling with *SCALA* were consistent with space group $P2_12_12$. Calculation of the Matthews coefficient indicated the presence of one molecule of RXLR3 within the asymmetric unit, with a V_M of 1.86 $Å^3$ Da^{-1} and a solvent content of 34%. RXLR3 required the presence of ammonium bromide to crystallize. As the diffraction data were collected at an X-ray wavelength close to the absorption peak of bromine, we hope to solve the structure using the SAD approach. Early indicators from scaling (*SCALA* output: ΔAnom correlation between half sets, Mid-Slope of Anom Normal Probability; Table 1) suggest the presence of anomalous signal in the data set collected.

We thank Dr Ruslan Yatusevich, Professor Jane Parker (Max-Planck Institute for Plant Breeding Research, Cologne), Dr Adriana Cabral and Professor Guido van den Ackerveken (Utrecht University) for providing the RXLR3 pENTR clone. We also thank Drs Alex Jones and Jan Sklenar (Sainsbury Laboratory) for mass spectrometry. This work was funded by a FEBS long-term fellowship (awarded to LW), by the Gatsby Charitable Foundation and by the BBSRC through the JIC core grant (MJB). We are grateful to the

beamline scientists for assistance with X-ray data collection at the Diamond Light Source.

References

Allen, R. L., Bittner-Eddy, P. D., Grenville-Briggs, L. J., Meitz, J. C., Rehmany, A. P., Rose, L. E. & Beynon, J. L. (2004). *Science*, **306**, 1957–1960.

Allen, R. L., Meitz, J. C., Baumber, R. E., Hall, S. A., Lee, S. C., Rose, L. E. & Beynon, J. L. (2008). *Mol. Plant Pathol.* **9**, 511–523.

Battye, T. G. G., Kontogiannis, L., Johnson, O., Powell, H. R. & Leslie, A. G. W. (2011). *Acta Cryst.* D**67**, 271–281.

Berrow, N. S., Alderton, D., Sainsbury, S., Nettleship, J., Assenberg, R., Rahman, N., Stuart, D. I. & Owens, R. J. (2007). *Nucleic Acids Res.* **35**, e45.

Boutemy, L. S., King, S. R. F., Win, J., Hughes, R. K., Clarke, T. A., Blumenschein, T. M. A., Kamoun, S. & Banfield, M. J. (2011). *J. Biol. Chem.*, doi:10.1074/jbc.M111.262303.

Cabral, A., Stassen, J. H., Seidl, M. F., Bautor, J., Parker, J. E. & Van den Ackerveken, G. (2011). *PLoS One*, **6**, e19328.

Chou, S., Krasileva, K. V., Holton, J. M., Steinbrenner, A. D., Alber, T. & Staskawicz, B. J. (2011). *Proc. Natl Acad. Sci. USA*, **108**, 13323–13328.

Dou, D., Kale, S. D., Wang, X., Jiang, R. H. Y., Bruce, N. A., Arredondo, F. D., Zhang, X. & Tyler, B. M. (2008). *Plant Cell*, **20**, 1930–1947.

Eitas, T. K. & Dangl, J. L. (2010). *Curr. Opin. Plant Biol.* **13**, 472–477.

Emanuelsson, O., Brunak, S., von Heijne, G. & Nielsen, H. (2007). *Nature Protoc.* **2**, 953–971.

Evans, P. (2006). *Acta Cryst.* D**62**, 72–82.

Fabro, G. *et al.* (2011). Submitted.

Lipka, V., Dittgen, J., Bednarek, P., Bhat, R., Wiermer, M., Stein, M., Landtag, J., Brandt, W., Rosahl, S., Scheel, D., Llorente, F., Molina, A., Parker, J., Somerville, S. & Schulze-Lefert, P. (2005). *Science*, **310**, 1180–1183.

Mukhtar, M. S. *et al.* (2011). *Science*, **333**, 596–601.

Panstruga, R. & Dodds, P. N. (2009). *Science*, **324**, 748–750.

Slusarenko, A. J. & Schlaich, N. L. (2003). *Mol. Plant Pathol.* **4**, 159–170.

Sohn, K. H., Lei, R., Nemri, A. & Jones, J. D. G. (2007). *Plant Cell*, **19**, 4077–4099.

Whisson, S. C., Boevink, P. C., Moleleki, L., Avrova, A. O., Morales, J. G., Gilroy, E. M., Armstrong, M. R., Grouffaud, S., van West, P., Chapman, S., Hein, I., Toth, I. K., Pritchard, L. & Birch, P. R. (2007). *Nature (London)*, **450**, 115–118.

Yaeno, T., Li, H., Chaparro-Garcia, A., Schornack, S., Koshiba, S., Watanabe, S., Kigawa, T., Kamoun, S. & Shirasu, K. (2011). *Proc. Natl Acad. Sci. USA*, **108**, 14682–14687.

Yang, Z. R., Thomson, R., McNeil, P. & Esnouf, R. M. (2005). *Bioinformatics*, **21**, 3369–3376.